PHONON DISPERSION ABOVE THE PEIERLS STRUCTURAL TRANSITION IN TTF-TCNQ ORGANIC CRYSTALS

Silvia Andronic and Anatolie Casian

Technical University of Moldova, Stefan cel Mare Avenue 168, Chisinau, MD-2004 Republic of Moldova
E-mail: andronic_silvia@yahoo.com

(Received May 12, 2016)

Abstract

The softening of acoustic phonons above the Peierls structural transition in quasi-one-dimensional (Q1D) TTF-TCNQ organic crystals is studied. Unlike other papers, a more complete physical model is applied to consider simultaneously two the most important electron−phonon interactions. The first is similar to that of deformation potential, and the second one is of polaron type. Analytic expressions for the phonon Green function and for the phonon polarization operator are obtained in the random phase approximation. The effects of interchain interaction on the phonon dispersion and Peierls critical temperature are analyzed.

Introduction

In recent years, investigation of quasi-one-dimensional (Q1D) organic crystals has excited special interest. These materials exhibit unusual properties [1–3]. In addition, low dimensionality of these structures, which can be considered almost one dimensional, makes them an ideal bench for testing theoretical models. Organic nanomaterials have large potential applications in electronics, sensing, energy-harnessing, and quantum-scale systems [4]. It has been also demonstrated that the highly conducting Q1D organic crystals may have very promising thermoelectric applications [5–7]. The most studied Q1D organic crystals are those of the tetrathiofulvalinium tetracyanoquinodimethane (TTF-TCNQ) type. However, not all parameters of this material are well determined. In this paper, we propose to use the Peierls structural transition to provide a more accurate determination of some parameters of this crystal.

This phenomenon has been theoretically predicted by Rudolf Peierls. According to Peierls, at some lowered temperatures, a one-dimensional metallic crystal with a half filled conduction band has to pass in a dielectric state with a dimerized crystal lattice. This temperature is referred to as the Peierls critical temperature. The Peierls transition has been studied by many authors (see [8–12] and references therein).

Recently, the physical model of Q1D organic crystals has been completed by an additional electron-phonon interaction mechanism. It takes into account the fluctuations due to acoustic longitudinal phonons of the polarization energy of molecules surrounding the conduction electron [13–15].

In [16], the Peierls structural transition in Q1D crystals of TTF-TCNQ type was investigated in a 1D approximation. Renormalized acoustic phonon frequencies $\Omega(q)$ as functions

of wave number q were calculated (i) provided that the conduction band is half filled and the dimensionless Fermi momentum $k_F = \pi/2$ and (ii) provided that the concentration of conduction electrons is reduced and the band is filled up to a quarter of the Brillouin zone, $k_F = \pi/4$. The Peierls critical temperature was established in both cases.

A 2D physical model for real TTF-TCNQ crystals was investigated in [17]. The effects of interchain interaction on the dispersion of renormalized phonons and on Peierls critical temperature were analyzed. The Peierls critical temperature was determined.

In [18], a 3D physical model of the crystal was studied. The Peierls transition was investigated for the case where the dimensionless Fermi momentum is $k_F = 0.59\pi/2$ for different values of parameters d_1 and d_2 which represents the ratio of the transfer energy in the transversal y and z directions to the transfer energy along the x direction of conductive chains. In addition, the polarization operator as a function of temperature was calculated for different values of increase or decrease δ in Fermi momentum k_F, which is determined by an increase or decrease in the carrier concentration. In this paper, the numerical modellings were performed for the sound velocity values at low temperatures taken from [19]: $v_{s1} = 3.4\cdot10^5$ cm/s along chains, $v_{s2} = 5.25\cdot10^5$ cm/s in the a direction and $v_{s3} = 5.25\cdot10^5$ cm/s in the c direction. However, more exact calculations showed that the sound velocity in the transversal direction cannot be higher the sound velocity along the chains.

The aim of this study is to present a detailed modeling of the Peierls transition in TTF-TCNQ crystals in a 3D approximation. The phonon Green function is calculated in the random phase approximation. The effects of interchain interaction on the dispersion of renormalized phonons and on Peierls critical temperature are analyzed. The results obtained in the 3D physical model are commented in detail.

1. Physical model in a 3D approximation

The structure and proprieties of TTF-TCNQ crystals are described in many papers (see [1] and references therein). A quasi-one-dimensional organic crystal of TTF-TCNQ is composed of TCNQ and TTF linear segregated chains. The TCNQ molecules are strong acceptors, and the TTF molecules are donors. Because the conductivity of TTF chains is much lower than that of TCNQ chains, we can neglect them in the first approximation. Thus, in this approximation, the crystal is composed of strictly one-dimensional chains of TCNQ that are packed in a three-dimensional crystal structure. The crystal lattice constants are a = 12.30 Å, b = 3.82 Å, and c = 18.47 Å, where b is in the chain directions.

The Hamiltonian of the 3D crystal in the tight-binding and nearest neighbor approximations has the form

$$H = \sum_{\boldsymbol{k}} \varepsilon(\boldsymbol{k}) a_{\boldsymbol{k}}^{+} a_{\boldsymbol{k}} + \sum_{\boldsymbol{q}} \hbar\omega_{\boldsymbol{q}} b_{\boldsymbol{q}}^{+} b_{q} + \sum_{\boldsymbol{k},\boldsymbol{q}} A(\boldsymbol{k},\boldsymbol{q}) a_{\boldsymbol{k}}^{+} a_{\boldsymbol{k}+\boldsymbol{q}} (b_{\boldsymbol{q}} + b_{-\boldsymbol{q}}^{+}), \tag{1}$$

In expression (1), $\varepsilon(\boldsymbol{k})$ represents the energy of a conduction electron with 3D quasi-wave vector $\boldsymbol{k}$ and projections (k_x, k_y, k_z), $a_{\boldsymbol{k}}^{+}$, $a_{\boldsymbol{k}}$ are the creation and annihilation operators of this electron. Carrier energy $\varepsilon(\boldsymbol{k})$ is measured from the conduction band bottom:

$$\varepsilon(\boldsymbol{k}) = 2w_1(1-\cos k_x b) - 2w_2(1-\cos k_y a) - 2w_3(1-\cos k_z c), \tag{2}$$

where w_1, w_2, and w_3 are the transfer energies of a carrier from one molecule to another along the

chain, *x* direction, and in perpendicular—*y* and *z*—directions. In (1), $b_{\boldsymbol{q}}^{+}$, $b_{\boldsymbol{q}}$ are the creation and annihilation operators of an acoustic phonon with three-dimensional wave vector $\boldsymbol{q}$ and frequency $\omega_{\boldsymbol{q}}$. The second term in Eq. (1) is the energy of longitudinal acoustic phonons

$$\omega_q^2 = \omega_1^2 \sin^2(q_x b/2) + \omega_2^2 \sin^2(q_y a/2) + \omega_3^2 \sin^2(q_z c/2), \tag{3}$$

where ω_1, ω_2, and ω_3 are the limit frequencies in the *x*, *y*, and *z* directions:

$$\omega_1 = \frac{2v_{s1}}{b},\ \omega_2 = \frac{2v_{s2}}{a},\ \omega_3 = \frac{2v_{s3}}{c}, \tag{4}$$

where v_{s1}, v_{s2}, and v_{s3} represent the values of the sound velocity at low temperatures along the chains (in *b* direction) and in perpendicular directions (in *a* and *c* directions).

The third term in Eq. (1) represents the electron–phonon interaction. It contains two important mechanisms. The first one is of the deformation potential type; it is determined by the fluctuations of energy transfer w_1, w_2, and w_3 due to the intermolecular vibrations (acoustic phonons). The coupling constants are proportional to derivatives w_1', w_2', and w_3' of w_1, w_2, and w_3 with respect to intermolecular distances, $w_1' > 0$, $w_2' > 0$, $w_3' > 0$. The second mechanism is similar to that of polaron. This interaction is conditioned by the fluctuations of the polarization energy of the molecules surrounding the conduction electron. The coupling constant of this interaction is proportional to the average polarizability of the molecule α_0. Because α_0 is roughly proportional to the volume of molecule, this interaction is important for crystals composed of large molecules, such as TCNQ.

The square module of the matrix element of electron–phonon interaction is represented in the following form:

$$\left|A(\boldsymbol{k},\boldsymbol{q})\right|^2 = 2\hbar w_1'^2/(NM\omega_{\boldsymbol{q}}) \times \{[\sin(k_x b) - \sin(k_x - q_x, b) + \gamma_1 \sin(q_x b)]^2 + \tag{5}$$

$$+ d_1^2[\sin(k_y a) - \sin(k_y - q_y, a) + \gamma_2 \sin(q_y a)]^2 + d_2^2[\sin(k_z c) - \sin(k_z - q_z, c) + \gamma_3 \sin(q_z c)]^2\},$$

In Eq. (5), M is the mass of the molecule, N is the number of molecules in the basic region of the crystal, $d_1 = w_2/w_1 = w_2'/w_1'$, $d_2 = w_3/w_1 = w_3'/w_1'$, parameters γ_1, γ_2, and γ_3 describe the ratio of amplitudes of the polaron-type interaction to the deformation potential one in the *x*, *y*, and *z* directions:

$$\gamma_1 = 2e^2\alpha_0/b^5 w_1',\ \gamma_2 = 2e^2\alpha_0/a^5 w_2',\ \gamma_3 = 2e^2\alpha_0/c^5 w_3', \tag{6}$$

To deduce an expression for a renormalized phonon Green function, we apply a random phase approximation. From exact series of the perturbation theory for the phonon Green function, we sum up the diagrams containing 0, 1, 2 …∞ closed loops of two electron Green functions that make the most important contribution. For the Fourier component of the phonon Green function $D(\boldsymbol{q}, \Omega)$, we obtain

$$D(\boldsymbol{q},\Omega) = D_0(\boldsymbol{q},\Omega) - D_0(\boldsymbol{q},\Omega)\Pi(\boldsymbol{q},\Omega)D(\boldsymbol{q},\Omega) \tag{7}$$

where $\Pi(\boldsymbol{q},\Omega)$ is the phonon polarization operator, $D_0(\boldsymbol{q},\Omega)$ is the free phonon Green function, $\boldsymbol{q}$ is the wave vector of longitudinal acoustic phonons, and $\Omega(\boldsymbol{q})$ is the renormalized phonon frequency. The real part of the polarization operator is presented in the form:

$$\mathrm{Re}\,\overline{\Pi}(\boldsymbol{q},\Omega) = -\frac{\overline{N}}{2\pi^3\hbar\omega_{\boldsymbol{q}}}\int_{-\pi}^{\pi}dk_x\int_{-\pi}^{\pi}dk_y\int_{-\pi}^{\pi}dk_z\left|A(\boldsymbol{k},-\boldsymbol{q})\right|^2\times\frac{n_{\boldsymbol{k}}-n_{\boldsymbol{k}+\boldsymbol{q}}}{\varepsilon(\boldsymbol{k})-\varepsilon(\boldsymbol{k}+\boldsymbol{q})+\hbar\Omega} \tag{8}$$

Hereinafter, $\boldsymbol{k}$ and $\boldsymbol{q}$ are dimensionless vectors, $\overline{N}$ represents the number of elementary cells in the basic region of the crystal, $N = r\overline{N}$, where r is the number of molecules in the elementary cell, $r = 2$. In (8), $A(\boldsymbol{k},\boldsymbol{-q})$ is the matrix element of electron–phonon interaction presented in Eq. (2), $\varepsilon(\boldsymbol{k})$ is the carrier energy, $\hbar$ is the Planck constant, $n_{\boldsymbol{k}}$ is the Fermi distribution function. $\Omega(\boldsymbol{q})$ is determined by the pole of function $D(\boldsymbol{q},\Omega)$ and is obtained from the transcendent dispersion equation

$$\Omega(\boldsymbol{q}) = \omega_{\boldsymbol{q}}[1-\overline{\Pi}(\boldsymbol{q},\Omega)]^{1/2} \tag{9}$$

This equation can be solved only numerically.

2. Results and discussion

Numerical modeling was performed for the following parameters of TCNQ chains: $M = 3.7\cdot10^5\ m_e$ (m_e is the electron rest mass), $w_1 = 0.125$ eV, $w_1' = 0.2$ eVÅ^{-1}, $a = 12.30$ Å, $b = 3.82$ Å, and $c = 18.47$ Å. The sound velocity $v_{s1} = 3.42\cdot10^5$ cm/s along chains, $v_{s2} = 1.7\cdot10^5$ cm/s in the a direction and $v_{s3} = 1\cdot10^5$ cm/s in the c direction, $d_1 = 0.015$, $d_2 = 0.013$, $r = 2$ (two molecules in a unit cell), $\gamma_1 = 1.37$. The γ_2 and γ_3 parameters are determined from the relationships: $\gamma_2 = \gamma_1 2^5 b^5/(a^5 d_1)$ and $\gamma_3 = \gamma_1 2^5 b^5/(c^5 d_2)$. The dimensionless Fermi momentum is $k_F = 0.59\,\pi/2$.

$$\mathrm{Re}\,\overline{\Pi}(\boldsymbol{q},\Omega) = \frac{w_1'^2}{8\pi^3 M w_1 r\omega_q^2}\int_{-\pi}^{\pi}dx\int_{-\pi}^{\pi}dy\int_{-\pi}^{\pi}dz\times$$

$$\times\Big[\frac{(\sin(x+q_x)-\sin(x)+\gamma_1\sin(q_x))^2+d_1^2(\sin(y+q_y)-\sin(y)+\gamma_2\sin(q_y))^2+}{\cos(x)-\cos(x+q_x)+d_1\cos(y)-d_1\cos(y+q_y)+} \tag{10}$$

$$\frac{+d_2^2(\sin(z+q_z)-\sin(z)+\gamma_3\sin(q_z))^2}{+d_2\cos(z)+d_2\cos(z+q_z)-\dfrac{\hbar\Omega}{2w_1}}\Big]\times(n_{\boldsymbol{k}}-n_{\boldsymbol{k}+\boldsymbol{q}}),$$

$$n_{\boldsymbol{k}} = [\exp(\frac{-2w_1\cos(x)-2w_2\cos(y)-2w_3\cos(z)+(2w_1+2w_2+2w_3)\cos(k_F)}{k_0T}+1)]^{-1}. \tag{11}$$

The polarization operator was calculated according to expression (10).

The dependences of renormalized phonon frequencies $\Omega(q_x)$ on q_x at different temperatures and different values of q_y and q_z are shown in Figs. 1–4. The same graphs show the same dependences for initial phonon frequency $\omega(q_x)$.

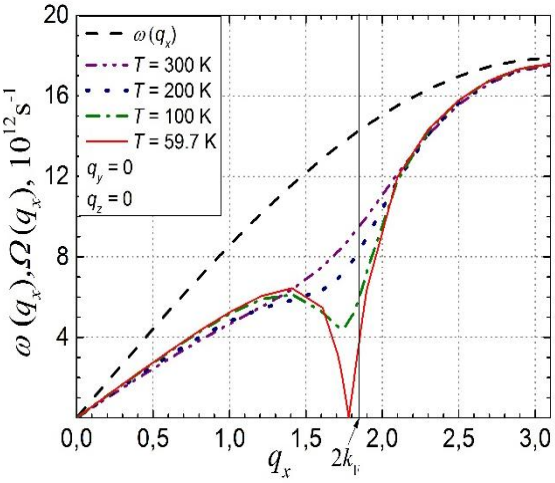

Fig.1. Renormalized phonon spectrum $\Omega(q_x)$ for $\gamma_1 = 1.37$ and different temperatures. The dashed line is for the spectrum of free phonons. $q_y = 0$ and $q_z = 0$.

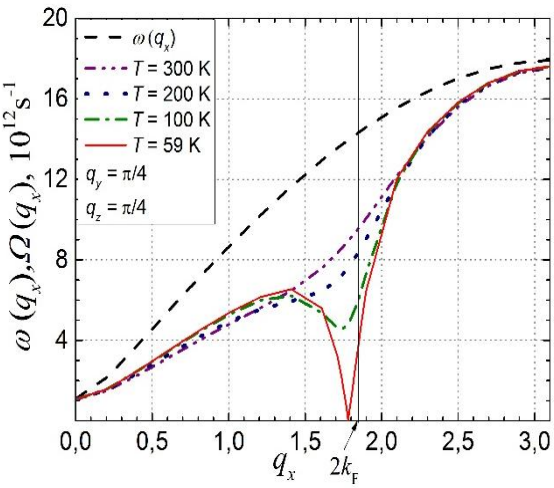

Fig.2. Renormalized phonon spectrum $\Omega(q_x)$ for $\gamma_1 = 1.37$ and different temperatures. The dashed line is for the spectrum of free phonons. $q_y = \pi/4$, $q_z = \pi/4$.

All figures show that the values of $\Omega(q_x)$ are diminished in comparison with those of frequency $\omega(q_x)$ in the absence of an electron–phonon interaction. This means that the electron–phonon interaction diminishes the values of lattice elastic constants. In addition, it is evident that, with a decrease in temperature T, the curves change their form. In dependences $\Omega(q_x)$, a minimum appears and becomes more pronounced at lower temperatures. It was expected that, at a certain temperature, $\Omega(q_x)$ will attain zero value for $q_x = 2k_F$. At this temperature, the structural Peierls transition should takes place. However, our calculations show that renormalized phonon frequencies $\Omega(q_x)$ attain zero value for $q_x = 0.58\pi$. This deviation from $q_x = 2k_F$ is caused by the deviation of k_F from $\pi/2$.

Figure 1 shows the phonon spectrum at $q_y = 0$ and $q_z = 0$. In this case, the last two terms in (5) become zero. This means that the interaction between TCNQ chains is not taken into account. The Peierls structural transition occurs in TCNQ chains alone at $T = 59.7$ K. The crystal lattice along TCNQ chains undergoes changes. A new crystalline state appears with lattice constant $4b$, which is four times larger. At this temperature, a metal–dielectric phase transition takes place, so as a gap in the carrier spectrum is fully open just above the Fermi energy. In addition, it is evident that the slope of $\Omega(q_x)$ at small q_x is diminished in comparison with that of $\omega(q_x)$. This means that the elasticity force of interaction between two nearest molecules as a consequence of electron–phonon interaction decreases. As a result, the sound velocity along the chains is diminished in a large temperature interval.

Figures 2–4 correspond to $q_y \neq 0$ and $q_z \neq 0$. It is observed that, if the interaction between TCNQ chains is taken into account ($q_y \neq 0$, $q_z \neq 0$), the Peierls critical temperature is diminished.

Figure 2 shows the $\Omega(q_x)$ dependences for $q_y = \pi/4$ and $q_z = \pi/4$ and different temperatures. One can observe that $\Omega(q_x)$ attains zero value at $T \sim 59$ K; that is, the Peierls transition takes place at this T.

Figure 3 shows the phonon spectrum at $q_y = 2k_F$ and $q_z = 2k_F$. It is evident from the graph that the Peierls critical temperature decreases further and has a value of $T \sim 56$ K. Figure 4 shows the dependences of $\Omega(q_x)$ on q_x for $q_y = \pi$, $q_z = \pi$ and different temperatures. It is observed that the transition temperature decreases even more significantly and has a value of $T \sim 54$ K. Note that this value corresponds to the experimental data.

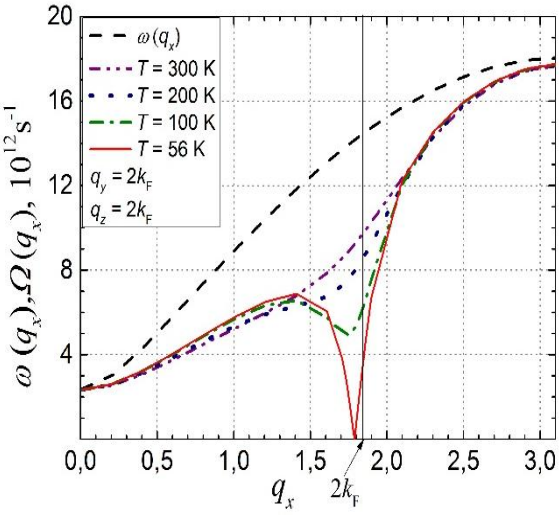

Fig.3. Renormalized phonon spectrum $\Omega(q_x)$ for $\gamma_1 = 1.37$ and different temperatures. The dashed line is for the spectrum of free phonons. $q_y = 2k_F$, $q_z = 2k_F$.

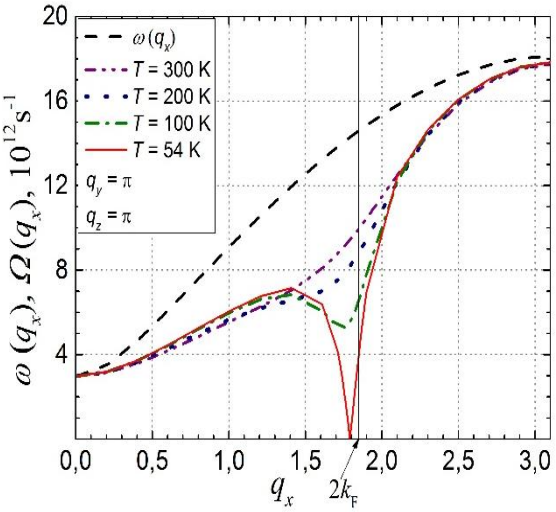

Fig.4. Renormalized phonon spectrum $\Omega(q_x)$ for $\gamma_1 = 1.37$ and different temperatures. The dashed line is for the spectrum of free phonons. $q_y = \pi$, $q_z = \pi$.

3. Conclusions

We have studied the effect of the Peierls transition on the phonon spectrum in quasi-one-dimensional organic crystals of TTF-TCNQ in a 3D approximation. A more complete crystal model has been applied to take into account two the most important electron–phonon interactions. One of them is of the deformation potential type. The other interaction is similar to that of a polaron. The ratio of amplitudes of the second electron–phonon interaction to the first one along the chains and in the transversal direction is denoted by γ_1, γ_2, and γ_3, respectively. Analytical expressions for the polarization operator and for the renormalized phonon Green function have been derived in a random phase approximation. Numerical calculations for renormalized phonon spectrum $\Omega(q_x)$ at different temperatures have been presented. It has been found that, at $q_y = 0$ and $q_z = 0$, if the interaction between TCNQ chains is neglected, the Peierls transition begins at $T \sim 59.7$ K (as confirmed experimentally) in TCNQ chains alone and reduces considerably the electric conductivity. Due to interchain interaction, the transition is completed at $T \sim 54$ K. It has been shown that the electron–phonon interaction diminishes $\Omega(q_x)$ and reduces the sound velocity in a large temperature interval. The frequency $\Omega(q_x)$ is about zero for $q_x = 0.58\pi$. The crystal

lattice changes from the initial state with lattice constant *b* to a new crystalline state with constant 4*b*.

Acknowledgments. The authors acknowledge the support of the scientific program of the Academy of Sciences of Moldova under project no. 14.02.116F.

References

[1] D. Jerome, J. Supercond. Novel Magn. 25, 633, (2012).
[2] J. P. Pouget, Physica B 407, 1762, (2012).
[3] X. Sun , L. Zhang , C. a. Di , Y. Wen , Y. Guo , Y. Zhao , G. Yu , and Y. Liu , Adv. Mater., 23 , 3128, (2011).
[4] Organic Nanomaterials: Synthesis, Characterization, and Device Applications (ed. by T. Torres, G. Bottari), John Wiley & Sons, Inc., Hoboken, NJ, USA, 2013.
[5] A. Casian., Thermoelectric Handbook, Macro to Nano, Ed. by D. M. Rowe, CRC Press, Chapter 36, 2006.
[6] A.I Casian., J. Pflaum, and I. I. Sanduleac, J. Thermoel. 1, 16, (2015).
[7] K. Harada, M. Sumino, C. Adachi, S. Tanaka, and K. Miyazaki, Appl. Phys. Lett. 96, 253304, (2010).
[8] L. N. Bulaevskii, Usp. Fiz. Nauk 115, 263, (1975).
[9] M. Hohenadler, H. Fehske, and F.F. Assaad, Phys. Rev. B, 83, 115105, (2011).
[10] V. Solovyeva et al., J. Phys. D: Appl. Phys. 44, 385301, (2011).
[11] U. Bernstein, P. Chaikin, and P. Pincus , Phys. Rev. Lett. 34, 271, (1975).
[12] A. Chernenkaya, K. Medjanik, P. Nagel, M. Merz, S. Schuppler, E. Canadell, J. P. Pouget, and G. SchËonhense, Eur. Phys. J. B. 88: 13, (2015).
[13] A. Casian, V. Dusciac, and Iu. Coropceanu, Phys. Rev. B 66, 165404, (2002).
[14] A. Casian, Phys. Rev. B 81, 155415, (2010).
[15] I. Sanduleac, A. Casian, and J. Pflaum, J. Nanoelectron. Optoelectron., 9, 247, (2014).
[16] S. Andronic and A. Casian, Mold. J. Phys. Sci. 12, 3–4, 192, (2013).
[17] S. Andronic and A. Casian, Adv. Mater. Phys. Chem. 6, 4, 98, (2016).
[18] S. Andronic, Mold. J. Phys. Sci. 14, 1–2, 96, (2015).
[19] T. Tiedje and R. R. Haering, Solid State Commun., 23, 713, (1977).